

COMPOSITE ELECTROMAGNETIC SCATTERING FROM THE PLATE TARGET ABOVE A ONE-DIMENSIONAL SEA SURFACE: TAKING THE DIFFRACTION INTO ACCOUNT

Z.-S. Wu and J.-J. Zhang

School of Science
Xidian University
Xi'an 710071, China

L. Zhao

China Research Institute of Radiowave Propagation
Qingdao 266107, China

Abstract—The properties of composite electromagnetic scattering from a square conducting plate target above a one-dimensional sea surface are discussed with the diffraction of plate edge taken into account. The characteristics of electromagnetic scattering from the sea surface are investigated based on the Kirchhoff Approximation (KA). The backscattering field of a plate target is calculated with the method of higher equivalent edge currents. Besides, the method of equivalent edge currents (MEC), Physical Optics (PO) approximation and the reciprocity theorem method are combined to calculate the composite scattering field from the conducting plate target above a sea surface. The effect of the plate size, inclination, edge diffraction and the frequency of incident wave on the composite scattering field is analyzed.

1. INTRODUCTION

The composite scattering field from the target above a rough surface has been studied widely and of extensive applications in many fields. For instance, in the case of detecting the missile flying over the sea surface with the radar, it must consider the missile and sea surface

Corresponding author: Z.-S. Wu (wuzhs@mail.xidian.edu.cn).

as a whole [1–3]. Because the coupling scattering field between the sea surface and the target above it affects the characteristics of the target scattering echo seriously, it leads to false alarm and missing alarm which brings great difficulty to guide and track. Not only should the electromagnetic scattering of targets [4] and the rough surface [5] be taken into account respectively, but also the coupling scattering field between them. Its study has attracted much interest during recent years [3, 6, 7]. Chiu et al. [8] utilized the reciprocity theorem to solve the interaction between a dielectric cylinder and a slightly rough surface. Johnson et al. [9–11] studied the scattering from an object above or below rough surface using different methods. Pino et al. [12] researched the scattering from targets on ocean-like surfaces with the forward-backward method. Zhu et al. [13] calculated the EM scattering from a 2D PEC target above a PEC rough surface using an efficient hybrid MM-PO method combining UV technique. Some numerical algorithms such as Finite-Difference Time-Domain [14], Fast Fourier Transform, the Multi-pole Expansion method [15], the model-based retrieval algorithm [16] and the method of moments [17] have also become some popular approaches to the rough surface scattering research because of the advent of modern computers and the development of computational technology.

The most common method that has been used in the research of scattering from a target is the method of equivalent edge currents which has three different types such as the equivalent edge currents for PO diffracted field (POEEC), the equivalent edge currents for physical theory of diffraction (PTDEEC) and the equivalent edge currents for geometrical theory of diffraction (GTDEEC). Several years ago, Michaeli [18–20] derived the explicit expressions for equivalent edge currents for an arbitrary local wedge angle and arbitrary directions of illumination and observation. Ando et al. [21–24] used a new coordinate to novel expressions for not only fringe but also PO and GTD equivalent edge currents without any false singularities. Besides, Sunuhara et al. [25] calculated the scattering of polyhedron structures by separated equivalent edge current method based on Sikta et al. [26] who used the equivalent current concept to compute the scattering patterns of flat plate structures.

In this paper, the third-order PTDEEC is employed to calculate the backscattering field of a square plate. The MEC, PO and the reciprocity theorem are combined to numerically calculate the composite scattering field from the square conducting plate at low altitude above a one-dimensional sea surface. The dependence of it on plate size, inclination, diffraction and frequency is numerically discussed.

2. CALCULATION OF COMPOSITE SCATTERING FIELD FROM THE PLATE ABOVE A SEA SURFACE

It will divide into three parts to calculate the composite scattering field in the paper. First, the KA is employed to calculate the primary scattering field of the sea surface. Then, the scattering of a square conducting plate is simulated by the third-order PTDEEC. At last, the coupling scattering field between the plate and the sea surface are computed based on the MEC and the reciprocity theorem, which includes the secondary scattering field of the sea surface to the plate and the plate target to the sea surface.

2.1. Computation of Primary Scattering Field and Surface Current of a Sea Surface

Suppose that an incident wave of unit amplitude impinges on a one-dimensional sea surface, extending from $x = -L$ to $x = L$. Based on the Kirchhoff Approximation [27, 28], it gets scattering field as follows

$$E_q^{(s)}(r_0, t) = \frac{ik \exp(ikr_0)}{4\pi r_0} \int_{-L}^L (pf'_x(x, t) - q) \exp[-iv_x x - iv_z f(x, t)] dx \quad (1)$$

where

$$p = (1 - R) \sin \theta_i + (1 + R) \sin \theta_s \quad (2)$$

$$q = (1 + R) \cos \theta_s - (1 - R) \cos \theta_i \quad (3)$$

$$v_x = k(\sin \theta_i - \sin \theta_s) \quad (4)$$

$$v_z = -k(\cos \theta_i + \cos \theta_s) \quad (5)$$

where θ_i and θ_s represent the incident and scattering angle respectively, k is the wavenumber of incident wave, r_0 is the distance from scattering center to the specular point, $f(x, t)$ is a descriptor function for the sea surface. For the backscattering, $\theta_s = -\theta_i$. R is the Fresnel reflection coefficient which can be expressed below in the vertical and horizontal polarization respectively

$$R_{vv} = \frac{\varepsilon_r \cos \theta_l - (\varepsilon_r - \sin^2 \theta_l)^{1/2}}{\varepsilon_r \cos \theta_l + (\varepsilon_r - \sin^2 \theta_l)^{1/2}}, R_{hh} = \frac{\cos \theta_l - (\varepsilon_r - \sin^2 \theta_l)^{1/2}}{\cos \theta_l + (\varepsilon_r - \sin^2 \theta_l)^{1/2}} \quad (6)$$

where ε_r is the relative dielectric constant, θ_l is the local incident angle. When the rough surface satisfies Kirchhoff approximation the surface current can be calculated by PO. With the TE plane wave, $\vec{E}_i = \hat{y} \exp(i\vec{k} \cdot \vec{r})$, surface equivalent current and magnetic current of

a one-dimensional sea surface can be expressed as follows respectively

$$\begin{aligned}\vec{J}_{rte} &= (1 - R_{hh})\hat{n} \times \vec{H}_i \\ &= (1 - R_{hh})\sqrt{\frac{\varepsilon}{\mu}} \frac{(\cos \theta_i + f'_x \sin \theta_i)}{\sqrt{1 + f_x'^2}} \exp(ikx \sin \theta_i - ikf \cos \theta_i) \hat{y}\end{aligned}\quad (7)$$

$$\begin{aligned}\vec{M}_{rte} &= -(1 + R_{hh})\hat{n} \times \vec{E}_i \\ &= (1 + R_{hh})\frac{\hat{x} + f'_x \hat{z}}{\sqrt{1 + f_x'^2}} \exp(ikx \sin \theta_i - ikf \cos \theta_i)\end{aligned}\quad (8)$$

where \hat{n} is the normal direction of the sea surface in free space, \vec{H}_i and \vec{E}_i represent magnetic and electric field of incident wave respectively. In the same way, it can also be calculated in TM polarization.

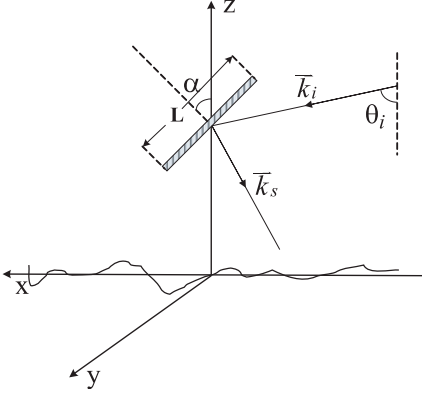


Figure 1. Illustration of composite scattering from the plate above sea surface.

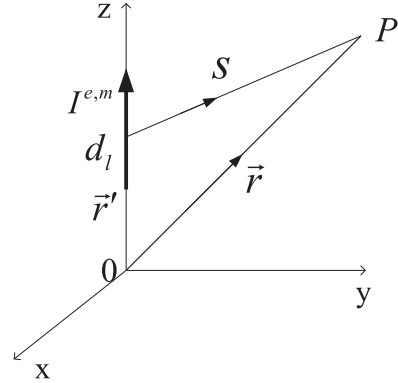


Figure 2. Illustration of radiation field of the method of equivalent edge currents.

2.2. Calculation of Primary Scattering Field of a Square Conducting Plate

The primary scattering field of the plate is calculated with the method of higher equivalent edge currents introduced in [29], when the incident wave, $\vec{E}_i = \hat{y} \exp(i\vec{k} \cdot \vec{r})$, illuminates a one-dimensional sea surface and a plate target as Fig. 1 shows, where $\vec{k}_i = k \sin \theta_i \hat{x} - k \cos \theta_i \hat{z}$, θ_i is the incident angle, \vec{k}_s is the scattering wave vector, L is the side length of the square plate, α is the angle between the normal direction of the

square plate and the forward direction of z axis. The coordinate of the plate centre is $(0, 0, z_0)$.

As shown in Fig. 2, according to the basic principle of the MEC, the radiation field can be expressed in an integral form

$$\vec{E}_s = ik_0 \int_C \left[\eta_0 I(\vec{r}') \hat{k}_s \times (\hat{k}_s \times \hat{t}) + M(\vec{r}') (\hat{k}_s \times \hat{t}) \right] \frac{\exp(-ik_0 S)}{4\pi S} dl \quad (9)$$

where the wave number of the incident wave can be defined as $k_0 = 2\pi/\lambda$, $\eta_0 = \sqrt{\frac{\mu_0}{\epsilon_0}}$ is the characteristic impedance of free space, \hat{k}_s is the wave vector of the scattered wave, \hat{t} is the tangential direction of the wedge edge, \vec{r}' is the position vector of one point on wedge edge, \vec{r} is the position vector of observation point and $S = |\vec{r}' - \vec{r}|$.

According to the document [29], I and M in formula (9) can be expressed in following

$$I_3^{PTD} = V_3 \frac{2 \exp(i\frac{\pi}{4})}{\sqrt{\pi}} \frac{1}{k_0 \beta_t^i} \{ [\cos(\beta_i + \beta_t^i) - \cos \beta_s \cos \beta_t^i] J_{x,A}^{PW}(0)(V_2 - V_1) + [\sin(\beta_i + \beta_s) + \cos \beta_s \sin \beta_s' \cos \varphi_s'] J_{z,A}^{PW}(0)V_1 \} \quad (10)$$

$$M_3^{PTD} = -\eta_0 V_3 \frac{2 \exp(i\frac{\pi}{4})}{\sqrt{\pi}} \frac{\sin \varphi_s \sin \beta_s}{k_0 \beta_t^i} [\sin(\beta_i + \beta_t^i) J_{x,A}^{PW}(0)(V_2 - V_1) - \cos(\beta_i + \beta_t^i) J_{x,A}^{PW}(0)V_1] \quad (11)$$

$$V_3 = \frac{\sin \beta_i}{\sin^2 \beta_s} \exp [ik_0 l (\sin \beta_s \cos \varphi_s \sin \beta_i + \cos \beta_s \cos \beta_i)] \quad (12)$$

$$V_2 = k_0 \sin \beta_t^i \int_0^{l'} \frac{\exp [-ik_0 \sigma' \sin \beta_t^i (\sin \beta_t^i - V_0)]}{\sqrt{2k_0 \sigma'} \sin \beta_t^i} d\sigma' \quad (13)$$

$$V_1 = -ik_0 \sin \beta_t^i \int_0^{l'} \exp [ik_0 \sigma' \sin \beta_t^i (\sin \beta_t^i + V_0)] F(\sqrt{2k_0 \sigma'} \sin \beta_t^i) d\sigma' \quad (14)$$

$$V_0 = \sin \beta_s' \cos \varphi_s' + \text{ctg} \beta_t^i (\cos \beta_s' - \cos \beta_t^i) \quad (15)$$

$$\cos \beta_s' = \sin(\beta_i + \beta_t^i) \cos \beta_s \cos \varphi_s + \cos(\beta_i + \beta_t^i) \cos \beta_s \quad (16)$$

$$\cos \varphi_s' = \frac{1}{\sin \beta_s'} [\cos(\beta_i + \beta_t^i) \sin \beta_s \cos \varphi_s - \sin(\beta_i + \beta_t^i) \cos \beta_s] \quad (17)$$

where I_3^{PTD} and M_3^{PTD} are current and magnetic current of the third-order equivalent edge currents for physical theory of diffraction. $J_{x,A}^{PW}(0)$ and $J_{z,A}^{PW}(0)$ represent the x -component and z -component of non-uniform current of edge A with the grazing incidence, respectively. In the Eq. (17), note that $\sin \beta_s'$ is zero in certain case, so the method exists oddity point. $l' = 0$ or uncertain will be occurred to the plate

with acute angle. Each parameter in formula (10)–(17) is shown in Fig. 3 and Fig. 4.

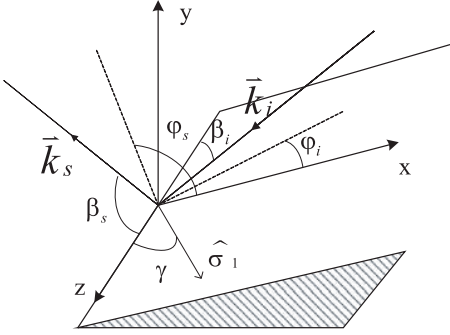


Figure 3. Illustration of wedge scattering.

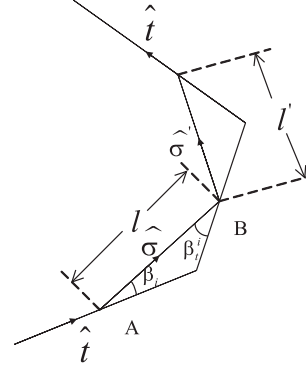


Figure 4. Illustration of non-uniform currents.

2.3. Calculation of Coupling Scattering Field

The TE plane wave, $\vec{E}_i = \hat{y} \exp(i\vec{k} \cdot \vec{r})$, impinging on the sea surface and plate target, the equivalent current of the sea surface are expressed in formula (7). The secondary scattering field, \vec{E}_{ph}^s , of plate target in hh polarization can be expressed in following according to the reciprocity theorem [8]

$$\begin{aligned}
 \hat{h} \cdot \vec{E}_{ph}^s &= \int_{S_1} \vec{J}_{rte} \cdot \vec{E}_{e22} dS \\
 &= \int_{s_1} (1 - R_{hh}) \sqrt{\frac{\varepsilon}{\mu}} \frac{(\cos \theta_i + f'_x \sin \theta_i)}{\sqrt{1 + f_x'^2}} \\
 &\quad \exp(-ikx \sin \theta_i + ikf \cos \theta_i) \hat{y} \cdot \vec{E}_{e22} dx \\
 &= (1 - R_{hh}) \sqrt{\frac{\varepsilon}{\mu}} \int_{s_1} \frac{(\cos \theta_i + f'_x \sin \theta_i)}{\sqrt{1 + f_x'^2}} \\
 &\quad \exp(-ikx \sin \theta_i + ikf \cos \theta_i) \hat{y} \cdot \vec{E}_{e22} dx \tag{18}
 \end{aligned}$$

In order to calculate \vec{E}_{ph}^s , we must compute \vec{E}_{e22} first which represents scattering field of plate target to a unit point electric current source.

Suppose there is a unit point electric current source $\vec{J}_e = \hat{y}\delta(\vec{r} - \vec{r}_0)$ at r_0 . The electric field stimulated in far-zone can be expressed as follows

$$\vec{E}_{ed}(\vec{r}) = \frac{ikZ_0}{4\pi r_0} \exp(ikr_0) \exp\left(-i\vec{k}_s \cdot \vec{r}\right) \hat{y} \quad (19)$$

Let $E_0 = \frac{ikZ_0}{4\pi r_0} \exp(ikr_0)$, where Z_0 is the characteristic impedance of free space, it attains

$$\vec{E}_{ed}(\vec{r}) = E_0 \exp\left(-i\vec{k}_s \cdot \vec{r}\right) \hat{y} \quad (20)$$

The incidence produced by point electric current source is expressed in the Eq. (20). The \vec{E}_{e22} can be calculated by the following formula

$$\vec{E}_{e22} = ik_0 \int_c \left[\eta_0 I(\vec{r}') \hat{k}_s \times (\hat{k}_s \times \hat{t}) + M(\vec{r}') (\hat{k}_s \times \hat{t}) \right] \frac{\exp(-ik_0 S)}{4\pi S} dl \quad (21)$$

where the meaning of each parameter is introduced in 2.2. By substitution of formula (21) into (18), it can obtain the secondary scattering field

$$\begin{aligned} & \hat{h} \cdot \vec{E}_{ph}^s \\ &= (1 - R_{hh}) \sqrt{\frac{\varepsilon}{\mu}} \int_{s_1} \frac{(\cos \theta_i + f'_x \sin \theta_i)}{\sqrt{1 + f'^2_x}} \exp(-ikx \sin \theta_i + ikf \cos \theta_i) \cdot \\ & ik_0 \int_c \left[\eta_0 I(\vec{r}') \hat{k}_s \times (\hat{k}_s \times \hat{t}) + M(\vec{r}') (\hat{k}_s \times \hat{t}) \right] \frac{\exp(-ik_0 S)}{4\pi S} dl dx \\ &= ik_0 (1 - R_{hh}) \sqrt{\frac{\varepsilon}{\mu}} \int_{s_1} \frac{(\cos \theta_i + f'_x \sin \theta_i)}{\sqrt{1 + f'^2_x}} \exp(-ikx \sin \theta_i + ikf \cos \theta_i) \cdot \\ & \int_c \left[\eta_0 I(\vec{r}') \hat{k}_s \times (\hat{k}_s \times \hat{t}) + M(\vec{r}') (\hat{k}_s \times \hat{t}) \right] \frac{\exp(-ik_0 S)}{4\pi S} dl dx \quad (22) \end{aligned}$$

Simultaneously, the secondary scattering field of the plate target in vv polarization can also be obtained.

2.4. Calculation of Total Field

The scattering field can be expressed as follows [8]

$$\vec{E}^s = [\exp(ikr)/r] \vec{S} \vec{E}^i \quad (23)$$

In which, \bar{S} is factor of scattering matrix. On account of the calculation results, the matrix components S_h , S_p and S_{hp} can be easily obtained, where the subscripts, h and p , represent sea surface and plate respectively. The matrix factor of coupling scattering can be obtained as follows [8]

$$\bar{S}_{hp}(\hat{k}_s, \hat{k}_i) = \bar{S}_{ph}^{(-t)}(-\hat{k}_i, -\hat{k}_s) \quad (24)$$

It can be expressed as matrix form in following

$$\begin{pmatrix} S_{hp}^{vv}(\hat{k}_i, \hat{k}_s) & S_{hp}^{vh}(\hat{k}_i, \hat{k}_s) \\ S_{hp}^{hv}(\hat{k}_i, \hat{k}_s) & S_{hp}^{hh}(\hat{k}_i, \hat{k}_s) \end{pmatrix} = \begin{pmatrix} S_{ph}^{vv}(-\hat{k}_s, -\hat{k}_i) & -S_{ph}^{hv}(-\hat{k}_s, -\hat{k}_i) \\ -S_{ph}^{vh}(-\hat{k}_s, -\hat{k}_i) & S_{ph}^{hh}(-\hat{k}_s, -\hat{k}_i) \end{pmatrix} \quad (25)$$

When we calculate backward coupling scattering field between the one-dimensional sea surface and plate, formula (24) can be simplified [8]

$$\begin{pmatrix} S_{hp}^{vv} & 0 \\ 0 & S_{hp}^{hh} \end{pmatrix} = \begin{pmatrix} S_{ph}^{vv} & 0 \\ 0 & S_{ph}^{hh} \end{pmatrix} \quad (26)$$

Based on above calculation results, the composite backscattering cross section is attained

$$\sigma = 4\pi |S_h + 2S_{ph} + S_p|^2 \quad (27)$$

The scattering cross section of coupling scattering is expressed as follows

$$\sigma_{ph} = 4\pi |2S_{ph}|^2 \quad (28)$$

3. NUMERICAL RESULTS

When the plate target perpendiculars to the sea surface, (i.e., $\alpha = 90^\circ$), the scattering field of the sea surface and the composite scattering field between the sea surface and the plate are shown in Fig. 5, taking the diffraction of the plate edge into account, where wavelength of incidence is 0.03 m, the distance between the center of the plate and the sea surface is 10 meters, the wind speed above the sea surface is 5 m/s, the dielectric constant of the sea is $\varepsilon = 20 - i5$ and the sea spectrum model is PM. It is worthy to note that the coupling field is the average field calculated based on 71 different sea surfaces.

From Fig. 5, it can draw the conclusion that with small incident angle the amplitude of composite scattering field is near to that of the sea surface so that the plate target can not be separated from the sea surface which mainly because the primary scattering field of

plate concentrate on specular direction and its adjacent domains. In case of small incident angle as shown in Fig. 1, the coupling domains

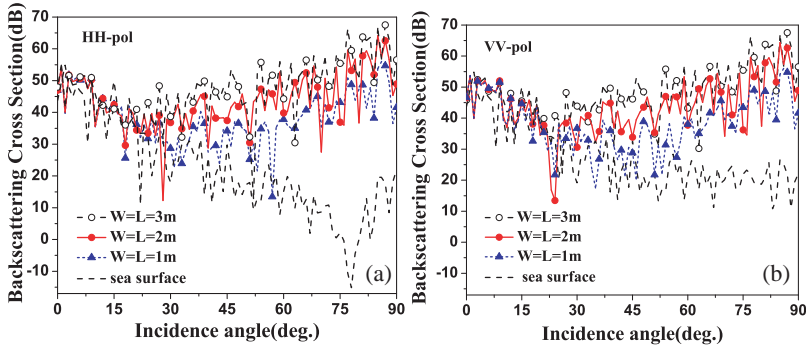


Figure 5. Illustration of composite scattering cross section between a sea surface and the plate with different sizes (W and L are width and length of the plate) taking diffraction of the plate edge into account, $\alpha = 90^\circ$.

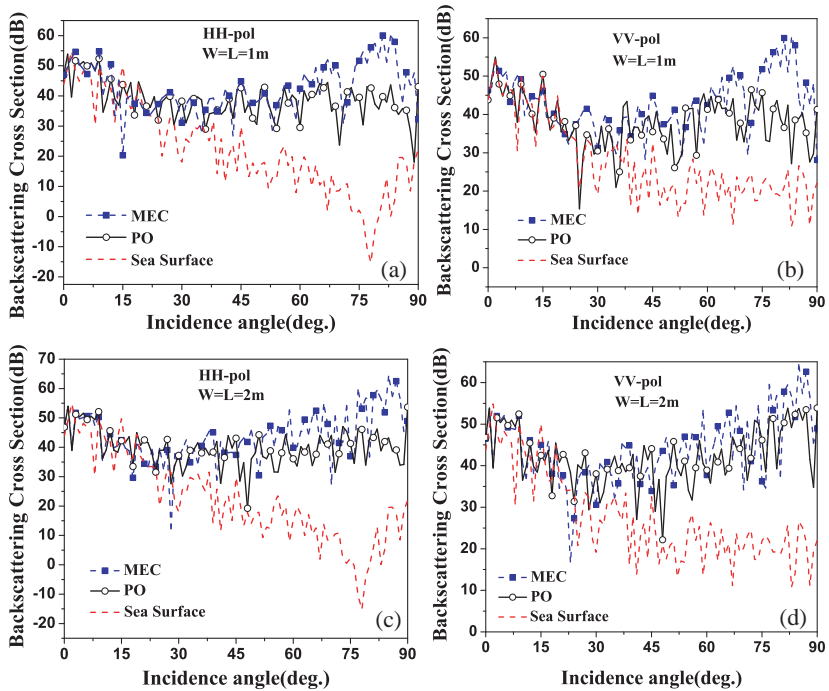


Figure 6. The comparison of composite backscattering cross section with and without diffraction.

between the plate and the sea surface are small so that the coupling scattering field has little contribution to composite scattering field. With the incident angle increased the coupling domains are larger and the coupling effect is enhanced, which leads to the separation of the plate target from the sea surface. Besides, with the increasing of plate size the composite scattering field increases evidently, which mainly because both the scattering intensity of the plate and the coupling scattering field increase with the plate size increased. It gets good agreement with Ref. [30]. And note that the coupling scattering field is calculated based on 71 different sea surfaces because the result cannot represent actual sea surface with one sample generated randomly which is so as to graphs below. However, with more than 71 samples the result has little variation.

Figure 6 gives the comparison of composite scattering between MEC and PO which is used in Ref. [30]. It gets conclusion that the composite scattering field calculated by MEC is larger than PO, because the integral domains of the sea surface are only specular direction and it has not considered the diffraction of plate edge and so

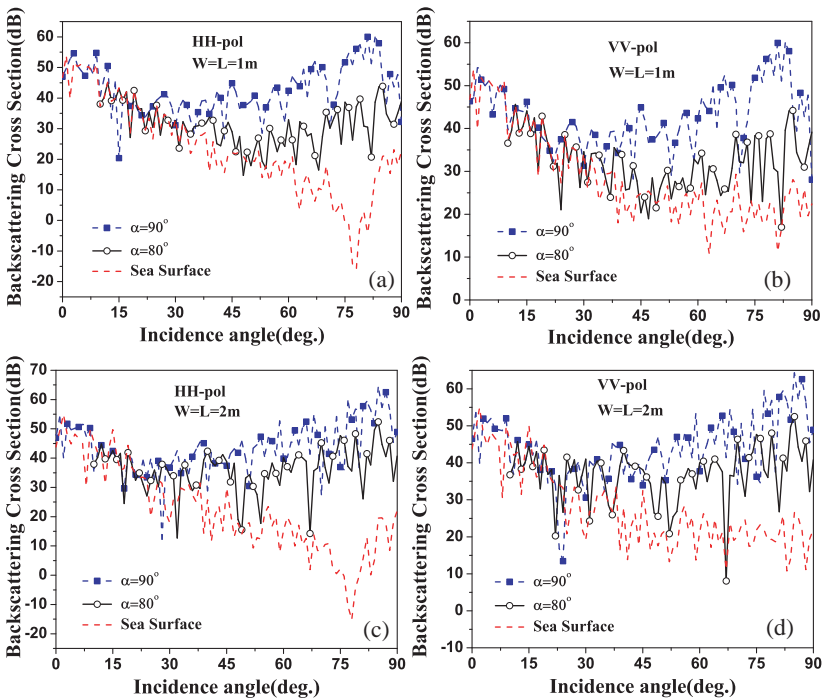


Figure 7. Illustration of comparison of composite backscattering cross section between $\alpha = 80^\circ$ and $\alpha = 90^\circ$.

as to the scattering field of the plate when calculate the composite scattering field by PO. Contrarily, when calculating the scattering field of plate target by MEC it has taken diffraction into account. In addition, MEC and the reciprocity theorem are combined to calculate coupling scattering field considering diffraction. Besides, integral domains are the whole sea surface so that the composite scattering field is larger than PO. From the analysis, in some condition, the diffraction of plate has much contribution to composite scattering field.

As shown in Fig. 7, the comparison of composite scattering field between $\alpha = 80^\circ$ and $\alpha = 90^\circ$ is shown without changing other parameters.

From Fig. 7, it can gain the conclusion that the composite scattering field of $\alpha = 90^\circ$ is larger than $\alpha = 80^\circ$, because the primary scattering field of plate concentrates mainly on specular direction for coupling scattering field. It is because of this point, when plate perpendiculars to sea surface, the specular direction of secondary scattering field of sea surface to plate target is just backward direction of composite scattering which makes the total field large and it gets good agreement with Ref. [30].

In Fig. 8, we can see that the composite backscattering cross section with 10 GHz is larger than 20 GHz, because with the frequency increased, the forward diffraction field of target's edge is larger, and the back-diffraction field of target's edge decreased [31], which also makes the coupling backscattering between the sea surface and the target weaken. As a result, the composite scattering field from the plate above the sea surface is reduced.

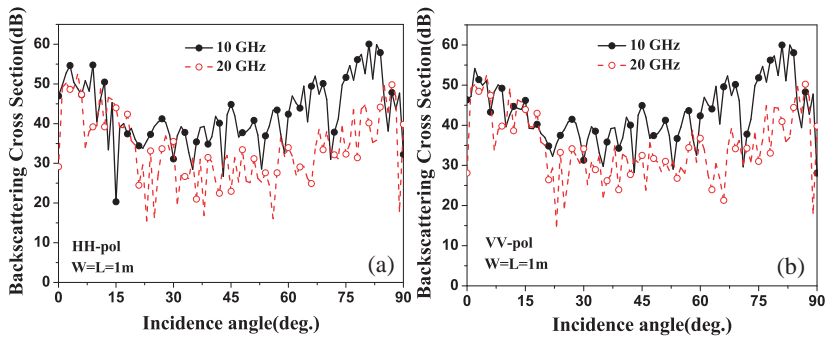


Figure 8. Illustration of composite backscattering cross section with different frequency.

4. CONCLUSION

MEC, PO and the reciprocity theorem are combined to calculate composite scattering field from a square conducting plate above a one-dimensional sea surface with varied sizes of the plate. The primary scattering field of a plate is calculated by third-order PTDEEC taking diffraction of plate edge into account. Especially, MEC and the reciprocity theorem are employed to calculate coupling scattering field with integral domains of the whole sea surface. The results of numerical calculation show that composite scattering cross section becomes larger with the plate size increased, which is affected by inclination angle. In the final analysis, in some condition, diffraction field has much contribution to composite scattering field. In addition, the incident wave is plane wave in the paper, which leads to edge effect caused by artificial truncated rough surface. In order to overcome the edge effect, the tapered incident wave will be employed in the future work. And, the results will be compared with the experimental data. Besides in actual situations, the impulse wave is used widely, such as radar detection. In order to increase more practicability, the composite scattering from a target above a sea surface will be studied in time domain with many methods in the future work such as time-domain equivalent edge current method (TD-EEC), time-domain physical optics (TD-PO), time-domain geometric theory of diffraction (TD-GTD), and time-domain uniform theory of diffraction (TD-UTD).

ACKNOWLEDGMENT

This work is supported by the National Natural Science Foundation of China (Grant No. 60371020 and No. 60771038).

REFERENCES

1. Ye, H.-X. and Y.-Q. Jin, "A hybrid analytic-numerical algorithm of scattering from an object above a rough surface," *IEEE Transactions on Geoscience and Remote Sensing*, Vol. 45, No. 5, 1174–1180, 2007.
2. Dehmollaian, M. and K. Sarabandi, "Electromagnetic scattering from foliage camouflaged complex targets," *IEEE Transactions on Geoscience and Remote Sensing*, Vol. 44, No. 10, 2698–2709, 2006.
3. Ye, H.-X. and Y.-Q. Jin, "Fast iterative approach to difference scattering from the target above a rough surface," *IEEE Transactions on Geoscience and Remote Sensing*, Vol. 44, No. 1, 108–115, 2006.

4. Li, Y.-L., J.-Y. Huang, et al., "The scattering cross section for a target irradiated by time-varying electromagnetic waves," *Journal of Electromagnetic Waves and Applications*, Vol. 21, No. 9, 1265–1271, 2007.
5. Wu, Z.-S., J.-P. Zhang, et al., "An improved two-scale model with volume scattering for the dynamic ocean surface," *Progress In Electromagnetics Research*, PIER 89, 39–56, 2009.
6. Kizilay, A. and E. Rothwell, "Efficient computation of transient TM scattering from a cylinder above an infinite periodic surface," *Journal of Electromagnetic Waves and Applications*, Vol. 13, No. 7, 943–961, 1999.
7. Kizilay, A. and E. J. Rothwell, "Transient multipath analysis of circular cylinders above sinusoidal surfaces using a ray tracing method," *Journal of Electromagnetic Waves and Applications*, Vol. 18, No. 1, 41–60, 2004.
8. Chiu, T. and K. Sarabandi, "Electromagnetic scattering interaction between a dielectric cylinder and slightly rough surface," *IEEE Transactions on Antennas and Propagation*, Vol. 47, No. 5, 902–913, 1999.
9. Johnson, J. T., "A numerical study of scattering from an object above a rough surface," *IEEE Transactions on Antennas and Propagation*, Vol. 50, No. 10, 1361–1367, 2002.
10. Johnson, J. T. and R. J. Burkholder, "A study of scattering from an object below a rough surface," *IEEE Transactions on Geoscience and Remote Sensing*, Vol. 42, No. 1, 59–66, 2004.
11. Johnson, J. T. and R. J. Burkholder, "Coupled canonical grid/discrete dipole approach for computing scattering from objects above or below a rough interface," *IEEE Transactions on Geoscience and Remote Sensing*, Vol. 39, No. 6, 1214–1220, 2001.
12. Pino, M. R., L. Landesa, J. L. Rodrigues, et al., "The generalized forward-backward method for analyzing the scattering from targets on ocean-like rough surfaces," *IEEE Transactions on Antennas and Propagation*, Vol. 47, No. 6, 961–968, 1999.
13. He, S.-Y. and G.-Q. Zhu, "A hybrid MM-PO method combining UV technique for scattering from two-dimensional target above a rough surface," *Microwave and Optical Technology Letters*, Vol. 49, No. 12, 2957–2960, 2007.
14. Moss, C. D., F. L. Teixeira, et al., "Finite-difference time-domain simulation of scattering from objects in continuous random media," *IEEE Transactions on Geoscience and Remote Sensing*, Vol. 40, No. 1, 178–186, 2002.

15. Johnson, B. R., "Calculation of light scattering from a spherical particle on a surface by the multi-pole expansion method," *Journal of the Optical Society of America A*, Vol. 13, No. 2, 326–337, 1996.
16. Chen, K.-S., T.-D. Wu, and J.-C. Shi, "A model-based inversion of rough soil surface parameters from radar measurements," *Journal of Electromagnetic Waves and Applications*, Vol. 15, No. 2, 173–200, 2001.
17. Wang, X., C.-F. Wang, Y.-B. Gan, and L.-W. Li, "Electromagnetic scattering from a circular target above or below rough surface," *Progress In Electromagnetics Research*, PIER 40, 207–227, 2003.
18. Michaeli, A., "Equivalent edge currents for arbitrary aspects of observation," *IEEE Transactions on Antennas and Propagation*, Vol. 32, No. 3, 252–258, 1984.
19. Michaeli, A., "Elimination of infinities in equivalent edge currents, Part I: Fringe current components," *IEEE Transactions on Antennas and Propagation*, Vol. 34, No. 7, 912–918, 1986.
20. Michaeli, A., "Equivalent currents for second-order diffraction by the edges of perfectly conducting polygonal surfaces," *IEEE Transactions on Antennas and Propagation*, Vol. 35, No. 2, 183–190, 1987.
21. Ando, M., T. Murasaki, et al., "Elimination of false singularities in GTD equivalent edge currents," *IEE Proceedings-H*, Vol. 138, No. 4, 289–296, 1991.
22. Murasaki, T. and M. Ando, "Equivalent edge currents by the modified edge representation: Physical optics components," *IEICE Transactions on Electronics*, Vol. E75-C, No. 5, 617–626, 1991.
23. Murasaki, T., et al., "Equivalent edge currents for the modified edge representation: Fringe wave components," *IEICE Transactions on Electronics*, Vol. E76-C, No. 9, 1412–1419, 1993.
24. Ando, M., K. Natsuhara, et al., "Pattern analysis of a GPS microstrip antenna on a rectangular ground plane by using modified edge representation," *IEICE Transactions on Communications*, Vol. E77-B, No. 6, 834–846, 1994.
25. Sunuhara, Y., et al., "Separated equivalent edge current method for calculating scattering cross section of polyhedron structures," *IEICE Transactions on Communications*, Vol. E-76B, No. 11, 1439–1444, 1993.
26. Sikta, F. A., et al., "First-order equivalent current and corner diffraction scattering from plate structures," *IEEE Transactions*

- on Antennas and Propagation*, Vol. 31, No. 4, 584–589, 1983.
27. Beckmann, P. and A. Spizzichino, “The scattering of electromagnetic waves from rough surfaces,” *Pergamon*, New York, 1963.
 28. Chen, J., K. Y. Lo, et al., “The use of fractals for modeling EM waves scattering from rough sea surface,” *IEEE Transactions on Geoscience and Remote Sensing*, Vol. 34, No. 4, 966–972, 1996.
 29. Cui, S.-M., Z.-S. Wu, and M.-G. Wang, “Generalized expressions for the first and higher equivalent edge currents and application in bistatic scattering,” *ACTA Electronica Sinica*, Vol. 26, No. 3, 43–47, 1998 (in Chinese).
 30. Guo, L.-X., Y.-H. Wang, and Z.-S. Wu, “Electromagnetic scattering interaction between a conducting plate and a 2-D conducting slightly rough surface,” *ACTA Physica Sinica*, Vol. 54, No. 11, 5130–5138, 2005 (in Chinese).
 31. Yu, X.-Q., “Analysis on back-diffraction field of target’s edge,” *Journal of Microwaves*, No. 4, 41–46, 1994 (in Chinese).